The Canadian Mineralogist
Vol. 37, pp. 1099-1115 (1999)

PLATINUM-GROUP MINERALS AS INDICATORS OF SULFUR FUGACITY IN OPHIOLITIC UPPER MANTLE: AN EXAMPLE FROM CHROMITITES OF THE RAY–IZ ULTRAMAFIC COMPLEX, POLAR URALS, RUSSIA

GIORGIO GARUTI[§]

Dipartimento di Scienze della Terra, Universitá di Modena, via S. Eufemia 19, I-41100 Modena, Italy

FEDERICA ZACCARINI

Dipartimento di Scienze della Terra e Geologico Ambientali, Università di Bologna, Piazza di Porta S. Donato 1, I-40126 Bologna, Italy

VASILY MOLOSHAG AND VICTOR ALIMOV

Russian Academy of Sciences, Ural Branch, Ekaterinburg, Str. Pochtovy per. 7, Ekaterinburg 620151, Russia

ABSTRACT

The Ray–Iz ophiolite complex (Polar Urals, Russia) contains large chromite deposits associated with concordant to discordant bodies of dunite emplaced within harzburgitic mantle tectonite. Primary inclusions (1–25 μm) of platinum-group-minerals (PGM) occur in the chromite, and consist of laurite, erlichmanite, and Os–Ir alloys, accompanied by cuproiridsite (Ir_2CuS_4), kashinite (Ir_2S_3), rhodian pentlandite, unknown sulfides with stoichiometries varying from $(Ni>Fe\geq Cu)_2(Ir>Rh)S_3$ to $(Ni>Fe\geq Cu)_2(Ir>Rh)S_4$, irarsite, cherepanovite (RhAs), and unknown $(Rh,Ni)_2As$. The PGM paragenesis indicates deposition through an unusually wide range of $f(S_2)$ and T compared with mantle-hosted chromitites from other ophiolite complexes. This wide range is ascribed to the crystallization of PGM and chromite down to a relatively low temperature (T), enabling the relative increase of $f(S_2)$. Such $f(S_2)$–T conditions, previously observed in chromitites of Tiebaghi (New Caledonia) and Kempirsai (southern Urals, Kazakhstan), seem to be peculiar to a chromite-forming system in fluid-metasomatized upper mantle of ophiolite complexes.

Keywords: platinum-group minerals, laurite, chromitite, sulfur fugacity, Ray–Iz complex, ophiolite, Polar Urals, Russia.

SOMMAIRE

Le complexe ophiolitique de Ray–Iz, dans les Ourales polaires, en Russie, contient des gisements importants de chromite associés à des massifs concordants ou discordants de dunite mis en place dans un manteau harzburgitique tectonisé. Des inclusions primaires (de 1 à 25 μm de diamètre) de minéraux du groupe du platine ont été trouvées dans la chromite: laurite, erlichmanite, et alliages de Os er d'Ir, qu'accompagnent cuproiridsite (Ir_2CuS_4), kashinite (Ir_2S_3), pentlandite rhodifère, des sulfures inconnus ayant une stoechiométrie entre $(Ni>Fe\geq Cu)_2(Ir>Rh)S_3$ et $(Ni>Fe\geq Cu)_2(Ir>Rh)S_4$, irarsite, cherepanovite (RhAs), et une phase encore inconnue, $(Rh,Ni)_2As$. L'association des minéraux du groupe du platine témoigne d'une cristallisation sur un intervalle assez grand de $f(S_2)$ et de T en comparaison des chromitites dans la partie mantellique d'autres complexes ophiolitiques. On attribue cet intervalle à la cristallisation des minéraux du groupe du platine et de la chromite jusqu'à des températures relativement faibles, ce qui a permis une fugacité de soufre relativement élevée. De telles conditions de $f(S_2)$–T, observées antérieurement dans les chromitites de Tiebaghi (Nouvelle-Calédonie) et Kempirsai (Ourales du sud, Kazakhstan), semblent typiques de milieux de formation de la chromite dans la séquence mantellique d'un complexe ophiolitique affecté par une métasomatose.

(Traduit par la Rédaction)

Mots-clés: minéraux du groupe du platine, laurite, chromitite, fugacité de soufre, complexe de Ray–Iz, ophiolite, Ourales polaires, Russie.

§ *E-mail address*: garutig@unimo.it

Introduction

There is now general agreement about the origin of inclusions of primary platinum-group minerals (PGM) in the chromite of chromitites. The PGM are considered as near-liquidus minerals trapped in the growing crystals of chromite. Their paragenesis and composition have frequently been used in the literature to estimate specific thermodynamic conditions, such as sulfur fugacity, $f(S_2)$, and temperature, T, prevailing in the magmatic system before and during the crystallization of chromite (Augé & Johan 1988, Nakagawa & Franco 1997, Garuti *et al.* 1999). The study of PGM inclusions in upper-mantle chromitites from a number of ophiolite complexes indicates that sulfur saturation was never reached, with sulfur fugacity usually well below the Os–OsS_2 buffer at temperatures above 1000°C. On the other hand, a few examples of chromite–PGM mineralization from ophiolitic mantle are known to have formed at relatively high $f(S_2)$ and low T. Among these are the Main Ore Field chromitites of the Kempirsai ophiolite massif, in the southern Urals (Melcher *et al.* 1997). The results of our investigation indicate that comparable conditions may have been achieved in the Ray–Iz complex of the Polar Urals. Economic deposits of chromite in the mantle section at Ray–Iz bear a strong similarity in geological setting and chromite composition to the Kempirsai chromitites (Makeyev *et al.* 1985, Koroteev *et al.* 1997). The potential of chromitites and ultramafic rocks for economic concentrations of platinum-group elements (PGE) was illustrated in a preliminary way by Volchenko (1990), whereas Anikina *et al.* (1996) described the composition of laurite occurring in dunite-hosted Cr-rich ores of the complex. In this paper, we report the discovery of PGM in chromitite samples obtained from exploration works in three major chromite deposits of the Ray–Iz complex, and document the existence of a complex association of PGM inclusions accompanying laurite. Results of a detailed study of the paragenesis and composition of the PGM are used to estimate conditions of $f(S_2)$ and T during chromite precipitation in the upper mantle section of the Ray–Iz ophiolite complex.

Geological Setting

Two major ophiolite belts, Khadatinsk and Voikar–Syninsk, occur in the Polar Urals, Russia (Savel'yev & Savel'yeva 1977, Sobolev & Dobretsov 1977, Efimov *et al.* 1978). They extend over a distance of more than 500 km, and are believed to represent fragments of a transition between the upper mantle and the crust, possibly exhumed from the Ordovician–Silurian lower oceanic lithosphere as a result of the closure of an ocean basin. Presently, the ophiolites are thrust over the European continental plate to the northwest, and in contact with intrusive and volcano-sedimentary units of the Silurian–Devonian island arc association to the east.

The Ray–Iz ultramafic massif (Fig. 1) extends between latitude 66°44' and 66°57' N, from longitude 65°09' to 65°44' E, covering an area of about 400 km^2 at the northeastern end of the Voikar–Syninsk ophiolite belt. It comprises the following units (Shmelev *et al.* 1990):

1) The mantle tectonite is about 15 km thick in its maximum exposed section, and appears to be composed of different types of ultramafic rocks. i) Massive harzburgite is characterized by intensive plastic deformation and tectonite fabric marked by the elongation of enstatite porphyroclasts, with fine bands of enstatite. ii) A dunite–harzburgite complex consists of harzburgite groundmass, including boudinaged lenses and discordant veins of dunite varying from a few meters up to several hundred meters in length. The dunite displays structural evidence of late formation and emplacement with respect to the host harzburgite. iii) Large bodies of massive, coarse-grained dunite occur in the dunite–harzburgite, usually intersecting the foliation and banding in the harzburgite. Around the bodies of massive dunite, the proportion of dunite veins and lenses in the dunite–harzburgite complex gradually increases from less than 10% to more than 50% by volume (Perevozchikov & Puchkov 1990), suggesting that the two types of dunite are genetically related. iv) Subconcordant to discordant clinopyroxenite and gabbroic dikes occur in the massive harzburgite and dunite–harzburgite complex (not shown in Fig. 1). v) Metamorphic equivalents of the ultramafic units, consisting of olivine – antigorite – chlorite schist and coarse-grained recrystallized olivine–enstatite rocks, occur in a narrow belt cutting across the mantle unit in a SW–NE direction, possibly marking a zone of discontinuity and relative movement between mantle blocks.

2) The ultramafic transition-zone is poorly developed in the Ray–Iz massif compared with the rest of the Voikar–Syninsk ophiolite belt. It consists of a layered body made up of dunite, wehrlite, and clinopyroxenite occurring next to the southwestern edge of the massif.

3) Supra-Moho mafic cumulates consist of an extensive sequence of gabbroic rocks, including blocks of the underlying ultramafic rocks, *i.e.*, harzburgite, dunite, and wehrlite. The gabbro unit is in tectonic contact with the ultramafic rocks of both the mantle unit and the transition zone along the southern border of the massif. It extends over some kilometers, passing eastward into diorites and amphibolites of an island arc association (not shown in Fig. 1).

4) A tectonic Mélange unit is mainly developed at the contact with Paleozoic metasedimentary and metavolcanic rocks in the northern part of the massif.

A sheeted dike complex and pillow lavas are absent in the Ray–Iz massif, although they do occur sporadically at the eastern margin of the ultramafic–mafic sequence in the southern part of the Voikar–Syninsk belt.

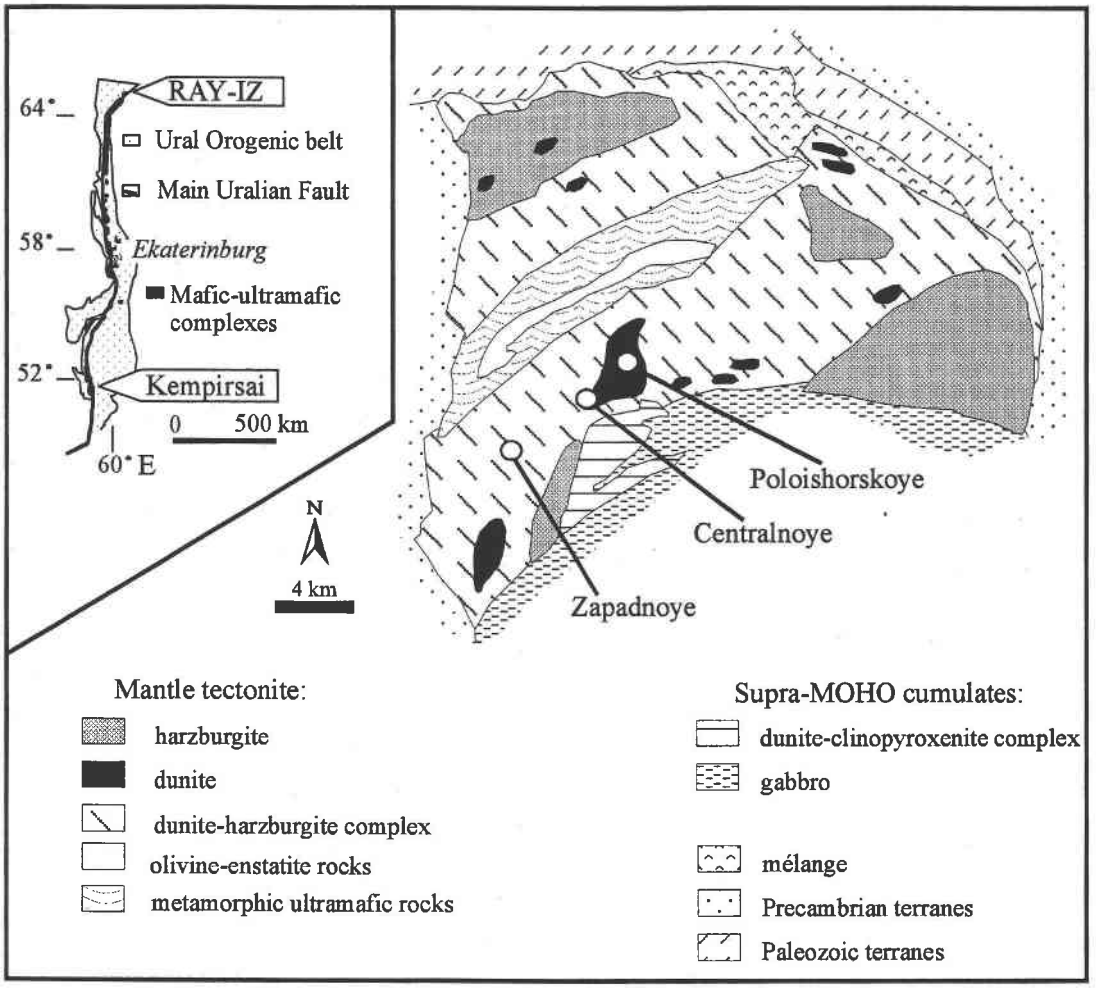

FIG. 1. Geological sketch-map of the Ray–Iz ophiolite complex (redrawn after Shmelev *et al.* 1990).

ANALYTICAL APPROACH

The PGM grains were located by scanning polished sections with the reflected light microscope at a magnification of 250–800×. Subsequently, they were analyzed with an ARL–SEMQ electron microprobe at the University of Modena, operated at an accelerating voltage of 15–27 kV and a beam current of 10–20 nA, with a beam diameter of less than 1 μm. Pure metals were used as standards for the PGE, whereas the peaks for S, As, and base metals were calibrated on synthetic NiAs, CoAsS, FeS_2, and $CuFeS_2$. The following X-ray lines were used in the analyses: $K\alpha$ for S, Fe, Cu and Ni, $L\alpha$ for Ir, Ru, Rh, Pt, Pd, and As, and $M\alpha$ for Os. Automatic corrections were performed for the interferences involving Ru–Rh, Ir–Cu, and Rh–Pd. Electron-microprobe analyses of grains smaller than 5 μm show totals as low as 90%, although calculation of atomic proportions allowed correct attribution to the mineral species in most cases. Back-scattered electron (BSE) images were obtained in the electron microscopy laboratory of the University of Granada, Spain.

CHROMITITES IN THE RAY–IZ MASSIF

Field relationships and sample locations

More than 200 podiform bodies of chromitite have been located in the Ray–Iz massif, spatially related with the various peridotite lithologies, and showing progressive increase of the Cr:Al ratio from harzburgite to dunite–harzburgite and massive dunites (Makeyev *et al.*

1985, Perevozchikov *et al.* 1990a). Reserves amounting to several tens of millions of tonnes of metallurgical grade chromite (53–65 wt% Cr_2O_3) are concentrated along the S–SW margin of the Ray–Iz massif, in a number of deposits related to large bodies of massive dunite and dunite lenses in the dunite–harzburgite complex. The chromitite samples examined (Table 1) come from boreholes and surface outcrops in the Poloishorskoye II (estimated reserves: 3.8 Mt), Centralnoye (18.2 Mt), and Zapadnoye (1.9 Mt) deposits (Fig. 1). Field relations, illustrated by the geological sketch-maps of the Centralnoye and Zapadnoye deposits (Figs. 2A, B), indicate that in this part of the complex, the chromitite occurs as SW–NE-trending lenses or tabular bodies, dipping about 70°–85°NW, within coarse-grained dunite.

TABLE 1. PROVENANCE OF THE SAMPLES INVESTIGATED

Locality	borehole	samples
Centralnoye	N 43	1398, 1399, 1400, 1401
	N 302	2243, 2246
	N 316	2375, 2399
	N 328	2309, 2344, 2356, 2364, 2365
Zapatanoye	N 21	2075, 2076, 2077, 2078, 2079 2081, 2083
Poloishorskoye II	(*)	2069, 4075, 4076, 4078 5016, 5081, 5083, 5825

(*): samples taken from surface outcrops.

Composition of the chromite

The chromite is usually fresh, although the more massive samples locally show fracturing and brecciation. Chemical zoning is limited to the development of a thin rim of ferrian chromite along grain boundaries and cracks (Perevozchikov *et al.* 1990a). The composition of unaltered chromite from the deposits investigated is remarkably homogeneous, the major oxides varying over the following ranges: Cr_2O_3: 52–62.2 wt%, Al_2O_3: 6.5–11.1%, MgO: 12.2–15.4%, and FeO_{tot}: 13.5–18.9%. The Fe_2O_3 content, calculated from results of electron-

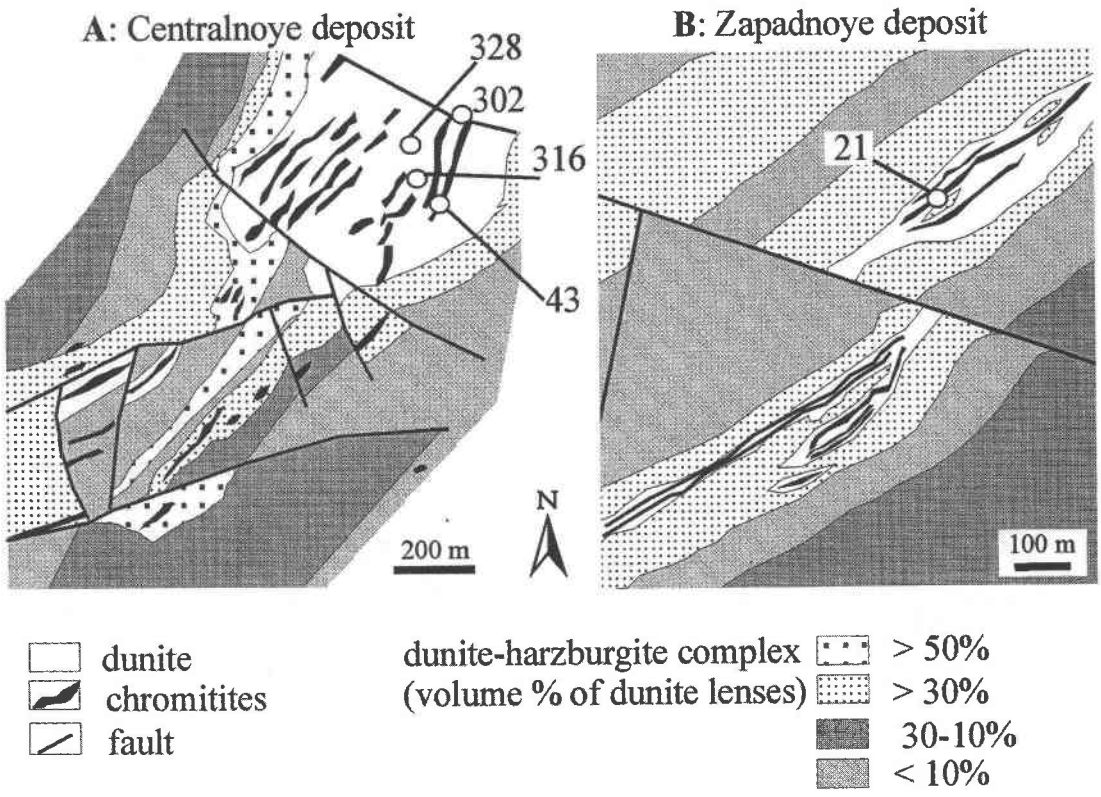

FIG. 2. Geological sketch-map of the Centralnoye (A) and Zapadnoye (B) chromite deposits (redrawn after Perevozchikov & Puchkov 1990). Location and numbers of the boreholes are indicated.

microprobe analyses assuming stoichiometry, is less than 5 wt%. Minor amounts of Ti (<0.2 wt% TiO_2), Mn (0.16–0.4% MnO), Ni (<0.25% NiO), V (0.09–0.24% V_2O_3) and Zn (0.08–0.46% ZnO) were detected. Compositional variations in terms of the diagram Cr/(Cr + Al) *versus* Fe/(Fe + Mg) display extreme enrichment in Cr and Mg, similar to the chromitites from the Main Ore Field of the Kempirsai ophiolite massif (Melcher *et al.* 1997, and our unpublished data: Fig. 3). The chromite-group mineral in this suite thus is magnesiochromite, but we will continue to refer to it below as "chromite" for convenience.

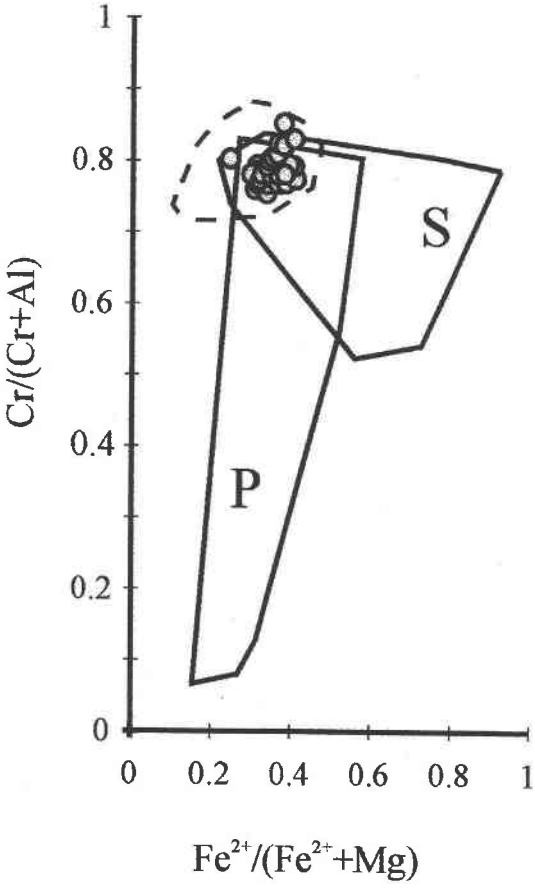

FIG. 3. Chemical composition of chromite from chromitites of the Ray–Iz complex projected in the Cr/(Cr + Al) *versus* Fe/(Fe + Mg) binary diagram. Dashed line: compositional field for chromitites from the Main Ore Field of Kempirsai (after Melcher *et al.* 1997, and unpublished data from the authors), P: field of podiform chromitite, S: field of stratiform chromitite.

Solid inclusions in chromite

Besides the PGM, a variety of primary solid inclusions have been observed in the unaltered chromite, and were identified by qualitative or quantitative electron-microprobe analysis. The most common inclusions are Ni–(Cu–Fe) sulfides and mafic silicates.

The sulfides occur as drop-like to euhedral grains (<30 μm) disseminated in the chromite, commonly associated with PGM and silicates. Millerite is the most abundant phase; also present are rare pentlandite, chalcopyrite, and a Cu-sulfide having the composition of digenite. Primary sulfides are distinguished from the secondary ones, which occur along cracks in association with ferrian chromite, and mainly consist of heazlewoodite and Ni-rich pentlandite.

Silicate inclusions consist of forsterite, clinopyroxene, pargasite, and chlorite up to 200 μm in size. One small grain (<50 μm) of Fe- and Cr-rich garnet was qualitatively identified. The forsterite is typically roundish, and is highly magnesian (Fo_{96-98}) compared with that of the host dunite and harzburgite (Fo_{88-93}). Olivine–spinel geothermometry (Sack & Ghiorso 1991) indicates a temperature of last equilibration with the including chromite in the range 650–740°C, thus much lower than the temperatures of 920–970°C calculated from forsterite–chromite pairs in the Ray–Iz harzburgites (Perevozchikov *et al.* 1990b). Clinopyroxene and pargasite commonly occur associated with PGM and are characterized by Na contents up to 0.7 and 5.2 wt% Na_2O, respectively. Chlorite is a common constituent of primary inclusions. It consists of tabular crystals commonly intergrown with clinopyroxene, pargasite, fresh chromite, and PGM (Figs. 4B, 5A–B), the texture suggesting that chlorite is a primary mineral, apparently unrelated with a processes of secondary alteration. The included chlorite is distinct from interstitial chromian chlinoclore, because of its Cr-poor and (Mg,Al)-rich composition, consistent with a relatively high temperature of stabilization, of the order of 700–800°C (Fawcett & Yoder 1966, Springer 1974).

THE PLATINUM-GROUP MINERALS

About a hundred PGM grains were discovered in chromitite samples from all the localities investigated. They are mainly Ru, Os, and Ir minerals comprising alloys, sulfides, sulfarsenides, arsenides and oxides (Table 2), and form primary, polygonal inclusions in fresh chromite, usually less than 15 μm across, but exceptionally reaching 50 μm in size. Only a few grains characterized by an irregular shape and a close association with secondary silicates are interpreted to have formed at a late stage, during low-temperature serpentinization and supergene alteration.

Ruthenium is present as laurite and rare, secondary Fe-rich Ru oxides. Osmium is present mainly as erlichmanite and Os–Ir–Ru alloys, and substitutes for

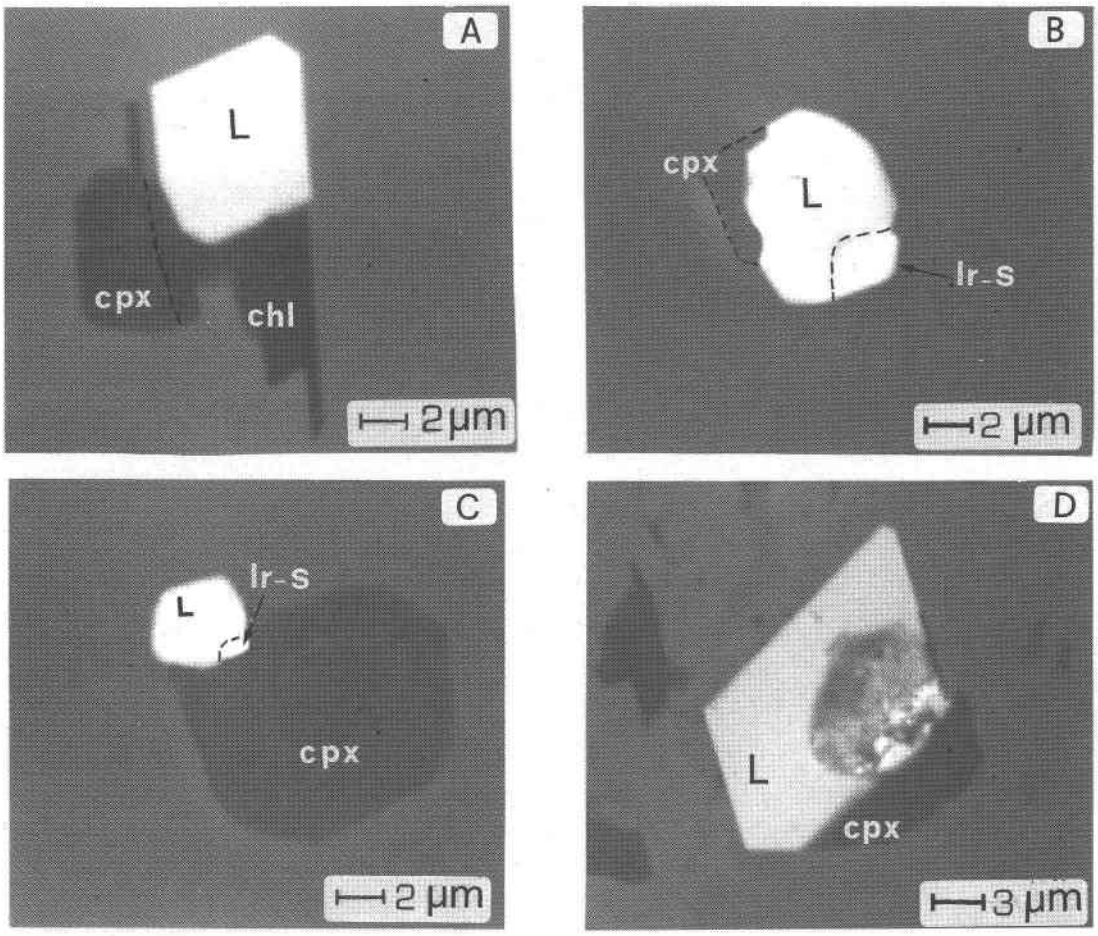

FIG. 4. Back-scattered electron (BSE) images showing textural relations of laurite-bearing primary composite inclusions. A) Idiomorphic laurite associated with clinopyroxene and chlorite in fresh chromite. B) and C) Laurite and Ir–Rh–Ni sulfide associated with clinopyroxene in fresh chromite. D) Laurite + clinopyroxene at the contact between fresh chromite and ferrian chromite + chlorite alteration rim. The laurite crystal appears corroded, and transformed into an indistinguishable aggregate of Ru–Ir–Ni–Os oxide (gray) and $(Ni,Rh)_2As$ (white). Labels: L: laurite, Ir–S: Ir–Rh–Ni sulfide, cpx: clinopyroxene, chl: chlorite.

Ru in the laurite and the oxide. Iridium is carried in solid solution in all the Ru and Os minerals; moreover, it forms specific sulfides (kashinite, cuproiridsite) and the sulfarsenide (irarsite). Iridium also is present as a major component of unknown Ir–Rh–Ni sulfides. Rhodium occurs as a minor constituent of laurite, erlichmanite, Ir sulfides, and rhodian pentlandite; it is, however, the major constituent of two arsenide minerals, cherepanovite and unknown $(Rh,Ni)_2As$. Both Pt and Pd generally occur in trace amounts, although up to 1–2 wt% Pt may occasionally be present in some cases. Examples of texture and paragenesis of the most common inclusions are shown in Figures 4 to 6. Selected microprobe compositions of PGM are reported in Tables 3 and 4.

THE Ru–Os–Ir SULFIDES AND ALLOYS

Laurite-erlichmanite series: ideally $(Ru,Os)S_2$

Laurite is by far the most abundant PGM encountered in the Ray–Iz chromitites. Compositions cover the entire range of Os-for-Ru substitution, and show a very high Ir content, even more than 15 wt% in Os-rich grains (anal. 2356–1, Table 3). The maximum Rh content observed in laurite is about 2 wt%. Some crystals are clearly zoned, showing a Ru-rich core and a marked increase of Os + Ir + Rh in the rim (anal. 2076–1C and 2076–1R, Table 3).

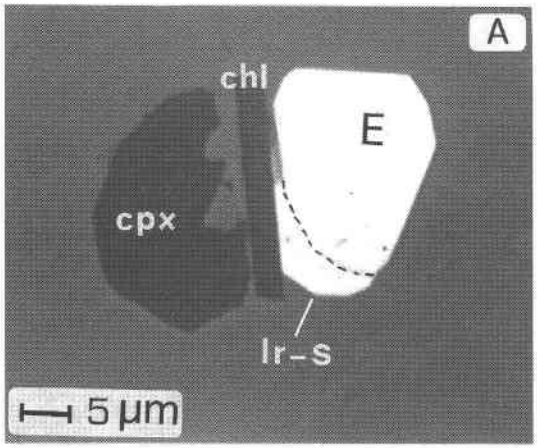

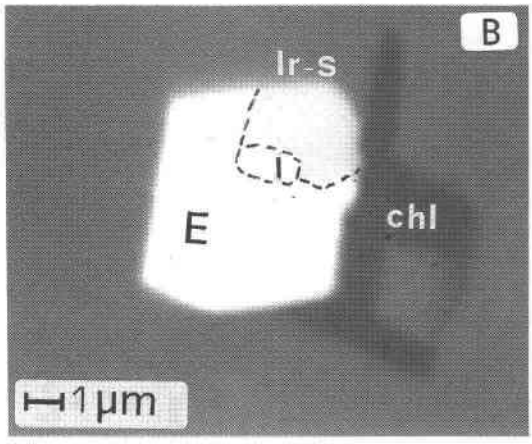

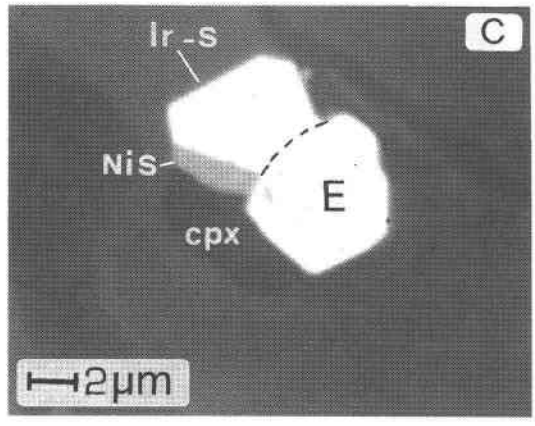

FIG. 5. BSE images showing textural relations of erlichmanite-bearing primary composite inclusions. A) Erlichmanite associated with Ir–Rh–Ni sulfide, chlorite, and clinopyroxene included in fresh chromite; an unidentified Cu-sulfide (medium grey) is located between chlorite and the PGMs. B) Erlichmanite associated with Ir–Rh–Ni sulfide, iridium, and chlorite, included in fresh chromite. C) Erlichmanite associated with Ir–Rh–Ni sulfide, millerite, and clinopyroxene in fractured chromite. Labels: E: erlichmanite, I: Iridium, NiS: millerite; others as in Figure 4.

TABLE 2. MINERALOGY OF THE PGM FROM RAY–IZ CHROMITITES

Sample	Deposits	PGM assemblage
1398	*Centralnoye*	laurite
1399	"	laurite, unknown Ir–Rh–Ni sulfide
1400	"	laurite, irarsite, unknown Ir–Rh–Ni sulfides, rhodian pentlandite
1401a	"	laurite
1401b	"	laurite, cuproiridsite, kashinite, unknown Ir–Rh–Ni sulfide
2243 a	"	laurite, Os–Ir alloy
2243 b	"	laurite, unknown Rh–Ni arsenide (*)
2246	"	laurite, irarsite
2344	"	laurite, unknown Ir–Rh–Ni sulfide
2356	"	laurite, unknown Ir–Rh–Ni sulfide
2375	"	laurite, Os–Ir alloy, unknown Ir–Rh–Ni sulfide
2399 a	"	laurite, unknown Ir–Rh–Ni sulfide
2399 b	"	laurite
2076	*Zapadnoye*	laurite, Os–Ir alloy
2077	"	laurite
2078	"	laurite, irarsite, cherepanovite
2079	"	laurite
2081a	"	laurite
2081b	"	laurite, irarsite
2083	"	laurite
4078	*Poloishorskoye II*	Ru–Os–Fe oxides (*)
5081	"	laurite (*), irarsite (*)
5825 a	"	laurite, Os–Ir alloy

(*) Secondary PGM.

One large grain of laurite, characterized by an irregular boundary and small inclusions of chromian chlorite, was observed in the altered silicate matrix (Fig. 6A). It has almost an end-member composition (anal. 5081a–1, Table 3) and is spotted with minute, drop-like exsolution-induced (?) blebs of irarsite (Fig. 6B). Both the laurite and the exsolved irarsite (anal. 5081a–1, Table 4) contain substantial Pt, up to 2.25 and 1.80 wt%, respectively. Because of its distinctive composition, morphology and paragenetic association, this sample of laurite is considered to have formed during low-temperature serpentinization.

Two groups of erlichmanite were identified. One is characterized by Ru-rich compositions, and follows the trend of Os-enrichment in laurite (*i.e.*, anal. 2344–3, Table 3, Fig. 7A). The other is characterized by extremely low Ru content and shows a clear trend of Os-for-Ir substitution, varying from Os-pure to Ir-rich erlichmanite (anal. 2375–2 and 2243a–1, Table 3). This latter composition represents the sulfide richest in Ir yet analyzed in the system Os–Ru–Ir; it was found in association with Os–Ir alloy.

TABLE 3. REPRESENTATIVE COMPOSITIONS OF Ru–Os–Ir MINERALS FROM THE RAY–IZ CHROMITITES

	Os	Ir	Ru	Rh	Pt	Pd	Ni	Fe	Cu	S	As	Total
						Weight % Element						
Laurite												
2076–1 C	1.72	2.98	57.63	0.02	0.00	0.21	0.06	0.00	0.29	35.79	0.00	98.70
2076–1 R	14.51	7.57	39.21	1.13	1.38	0.30	0.00	0.04	0.00	34.86	0.00	99.00
1399–5	10.10	7.76	43.60	0.89	0.13	0.03	0.41	0.38	0.06	37.37	0.00	100.73
1401a–2a	28.67	7.74	27.88	0.26	0.00	0.00	0.00	0.00	0.11	31.77	0.00	96.44
2079–1	22.91	13.48	28.03	0.78	0.00	0.24	0.05	0.53	0.04	31.83	0.00	97.89
2243b–2	10.29	7.57	46.31	1.48	0.00	0.00	0.08	0.00	0.00	36.83	0.00	102.56
2356–1	27.64	15.14	21.29	0.95	0.00	0.02	0.07	0.00	0.03	30.18	0.91	96.23
2375–6	32.11	12.68	24.83	1.10	0.00	0.00	0.16	0.03	0.13	32.06	0.00	103.10
2399a–2	28.42	13.12	27.35	0.70	0.00	0.00	0.19	0.02	0.16	31.58	0.00	101.54
2399b–1	22.34	6.97	33.24	0.23	0.00	0.15	0.10	0.03	0.00	34.52	0.00	97.57
5081a–1	1.34	0.50	55.72	1.12	1.80	0.37	0.12	0.18	0.00	38.89	0.00	100.04
Erlichmanite												
1401a–2a	42.52	8.79	9.82	1.57	0.00	0.66	0.16	0.00	0.00	27.25	1.25	92.02
2243a–1	48.22	17.13	1.87	0.25	0.00	0.00	0.09	0.00	0.00	24.01	0.72	92.29
2344–3	43.35	10.37	12.88	0.06	0.00	0.04	0.11	0.17	0.00	30.63	0.49	98.10
2375–2	65.92	1.23	0.22	0.07	0.07	0.23	2.08	0.00	0.00	26.67	0.39	96.88
2399b–1	63.92	10.30	1.18	0.07	0.00	0.00	0.30	0.00	0.00	24.62	0.02	100.40
Alloys												
2076–2	50.21	43.43	1.59	0.46	3.69	0.00	0.23	0.18	0.00	0.00	0.04	99.83
2243a–1	48.84	42.06	0.02	0.00	0.00	0.00	0.12	0.58	0.90	1.55	0.10	94.17
2375–4	56.31	40.32	0.01	0.18	0.00	0.00	0.00	0.00	0.00	0.00	0.04	96.86
2375–6	48.11	44.06	0.06	0.00	0.00	0.03	0.04	0.91	0.00	0.00	0.00	93.21
5825a–1	61.56	35.35	3.48	0.24	0.00	0.12	0.04	0.00	0.00	0.06	0.00	100.85
Ru–Os–Fe oxides												
4078–14	11.77	5.56	52.81	0.00	0.00	0.00	1.11	6.02	0.00	0.15	0.00	77.42
4078–5	5.90	4.92	57.57	0.03	0.00	0.00	0.98	10.73	0.00	0.00	0.00	80.13
						Atomic % Element						
Laurite												
2076–1 C	0.525	0.878	33.184	0.014	0.000	0.114	0.063	0.000	0.268	64.955	0.000	
2076–1 R	4.732	2.442	24.059	0.682	0.438	0.176	0.000	0.046	0.000	67.425	0.000	
1399–5	3.097	2.355	25.165	0.503	0.037	0.014	0.402	0.395	0.058	67.974	0.000	
1401a–2a	10.312	2.756	18.866	0.175	0.000	0.000	0.000	0.000	0.113	67.778	0.000	
2079–1	8.131	4.727	18.723	0.513	0.000	0.153	0.052	0.642	0.046	67.014	0.000	
2243b–2	3.153	2.295	26.698	0.840	0.000	0.000	0.082	0.000	0.000	66.932	0.000	
2356–1	10.405	5.638	15.079	0.659	0.000	0.015	0.088	0.000	0.033	67.385	0.868	
2375–6	11.283	4.410	16.421	0.712	0.000	0.000	0.178	0.037	0.137	66.822	0.000	
2399a–2	10.054	4.595	18.209	0.459	0.000	0.000	0.220	0.026	0.171	66.266	0.000	
2399b–1	7.505	2.317	21.019	0.143	0.000	0.088	0.103	0.036	0.000	68.789	0.000	
5081a–1	0.392	0.145	30.583	0.603	0.511	0.192	0.112	0.182	0.000	67.279	0.000	
Erlichmanite												
1401a–2a	17.784	3.638	7.732	1.211	0.000	0.494	0.220	0.000	0.000	67.599	1.323	
2243a–1	22.565	7.931	1.645	0.219	0.000	0.000	0.136	0.000	0.000	66.649	0.856	
2344–3	16.551	3.917	9.256	0.044	0.000	0.027	0.137	0.216	0.005	69.374	0.474	
2375–2	28.162	0.520	0.177	0.052	0.029	0.176	2.880	0.000	0.000	67.585	0.418	
2399b–1	28.597	4.562	0.990	0.055	0.000	0.000	0.431	0.000	0.000	65.344	0.022	
Alloys												
2076–2	49.191	42.103	2.928	0.838	3.523	0.000	0.714	0.593	0.000	0.000	0.109	
2243a–1	46.510	39.638	0.030	0.000	0.000	0.000	0.370	1.892	2.566	8.756	0.237	
2375–4	58.245	41.277	0.018	0.344	0.000	0.000	0.000	0.000	0.000	0.000	0.116	
2375–6	50.592	45.854	0.113	0.000	0.000	0.064	0.119	3.259	0.000	0.000	0.000	
5825a–1	59.079	33.570	6.286	0.426	0.000	0.199	0.121	0.000	0.000	0.319	0.000	
Ru–Os–Fe oxides												
4078–14	8.309	3.886	70.180	0.000	0.000	0.000	2.530	14.488	0.000	0.607	0.000	
4078–5	3.713	3.065	68.193	0.030	0.000	0.000	1.994	23.005	0.000	0.000	0.000	

Compositions pertaining to the same inclusion are indicated with the same label. C: core, R: rim.

TABLE 4. REPRESENTATIVE COMPOSITIONS OF Ir–Rh MINERALS FROM THE RAY–IZ CHROMITITES

	Os	Ir	Ru	Rh	Pt	Pd	Ni	Fe	Cu	S	As	Total
						Weight % Element						
Kashinite												
1401b–5	0.10	68.12	0.00	5.80	0.29	0.00	0.14	0.00	0.29	20.84	0.00	95.58
Cuproiridsite												
1401b–1	0.00	55.98	0.05	5.95	1.64	0.11	0.22	0.01	10.52	22.57	0.02	97.07
Rhodian pentlandite												
1400–4	0.12	0.00	0.00	7.42	0.00	0.53	41.54	14.00	0.00	31.49	0.34	95.44
1400–5	0.20	0.43	0.00	8.06	0.00	0.11	39.16	15.54	0.00	30.93	0.03	94.46
Unknown Ir–Rh–Ni sulfide												
1399–4	0.00	42.81	0.00	3.78	0.08	0.24	11.68	5.06	6.36	28.50	0.02	98.53
1399–5	0.58	34.33	0.61	5.45	0.00	0.00	15.17	7.64	5.55	30.53	0.07	99.93
1400–4	0.03	37.09	0.00	4.66	0.00	0.01	16.06	6.39	5.15	27.69	0.02	97.10
2344–3	0.17	41.73	0.00	0.36	0.83	0.00	16.99	5.16	5.06	29.54	0.00	99.84
2375–2	0.00	43.15	0.00	0.00	0.00	0.07	15.40	6.95	4.12	27.26	0.08	97.03
2399a–2	0.11	42.96	0.03	2.07	0.00	0.00	19.59	4.13	4.34	27.51	0.02	100.76
Irarsite												
1400–5	0.98	44.07	2.51	9.08	0.00	0.67	0.00	0.53	0.00	11.99	26.36	96.19
5081a–1	0.00	55.84	0.00	6.71	2.25	0.37	0.00	0.00	0.00	10.85	24.55	100.57
Cherepanovite												
2078–3	1.00	1.40	20.44	31.25	0.00	0.76	0.55	0.26	0.05	0.57	41.17	97.45
						Atomic % Element						
Kashinite												
1401b–5	0.050	33.138	0.000	5.269	0.138	0.000	0.215	0.000	0.428	60.763	0.000	
Cuproiridsite												
1401b–1	0.000	23.633	0.038	4.692	0.680	0.085	0.304	0.003	13.430	57.116	0.019	
Rhodian pentlandite												
1400–4	0.032	0.000	0.000	3.565	0.000	0.246	34.979	12.395	0.000	48.561	0.222	
1400–5	0.052	0.113	0.000	3.930	0.000	0.053	33.464	13.964	0.000	48.404	0.019	
Unknown Ir–Rh–Ni sulfide												
1399–4	0.000	14.455	0.000	2.385	0.027	0.148	12.907	5.875	6.494	57.687	0.021	
1399–5	0.181	10.655	0.360	3.158	0.000	0.000	15.416	8.166	5.209	56.802	0.054	
1400–4	0.011	12.280	0.000	2.881	0.000	0.008	17.405	7.288	5.158	54.954	0.014	
2344–3	0.057	13.496	0.000	0.220	0.264	0.000	17.985	5.745	4.951	57.282	0.000	
2375–2	0.000	14.692	0.000	0.000	0.000	0.042	17.168	8.149	4.245	55.631	0.072	
2399a–2	0.037	14.160	0.017	1.273	0.000	0.000	21.141	4.682	4.331	54.342	0.018	
Irarsite												
1400–5	0.473	21.051	2.283	8.101	0.000	0.581	0.000	0.878	0.000	34.323	32.312	
5081a–1	0.000	28.023	0.000	6.288	1.111	0.331	0.000	0.000	0.000	32.638	31.608	
Cherepanovite												
2078–3	0.048	0.658	18.333	27.535	0.000	0.643	0.843	0.425	0.074	1.615	49.825	
Unknown Rh–Ni arsenide												
2243b–2	0.368	2.389	5.496	26.329	0.000	0.493	30.081	0.000	0.000	1.781	33.062	

Abbreviations as in Table 3.

Os–Ir–Ru alloy

The Os–Ir–Ru alloy usually forms euhedral crystals not larger than 5 μm across. Compositions exhibit low Ru and high Ir contents, and range from $Os_{59.7}Ir_{33.9}Ru_{6.4}$ to $Os_{53.9}Ir_{46}Ru_{0.1}$ (anal. 5825a–1 and 2243a–1, Table 3); they are attributed to the species osmium (Harris & Cabri 1991). Variable amounts of Pt, Fe, Cu, S, and As have been occasionally detected in the grains of alloy. Minute grains of an Ir alloy were encountered in composite inclusions with erlichmanite and Ir–Rh sulfides (Fig. 5B). They could not be analyzed because of their small size (<1 μm), although semiquantitative analyses give compositions deduced from X-ray spectra that are

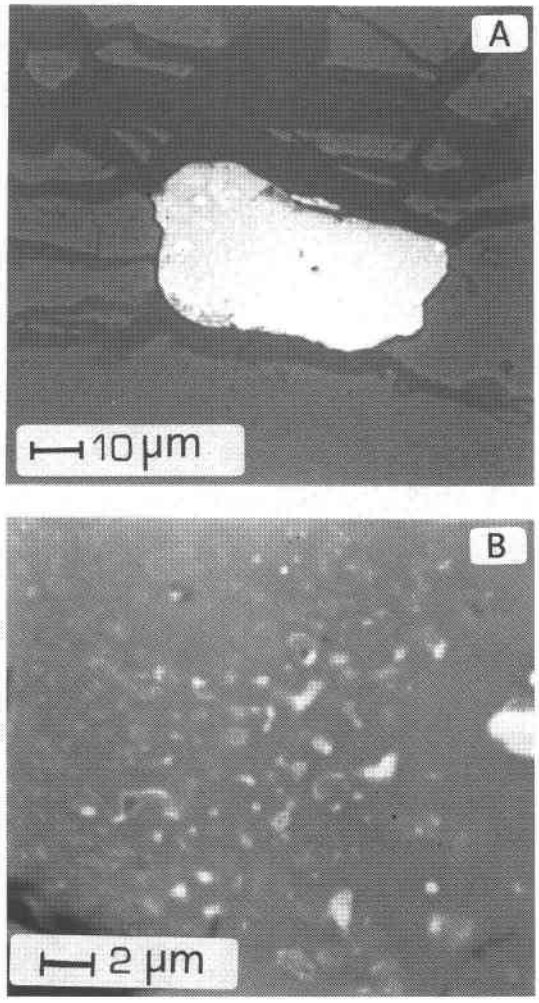

FIG. 6. BSE images showing a large grain of secondary laurite (A) characterized by an irregular boundary in contact with chromian clinochlore (black) and chlorite-pitted ferrian chromite (grey). The grain of laurite contains two small inclusions of chromian clinochlore, whereas minute exsolution-induced (?) blebs of Pt-rich irarsite occupy the entire body of the grain (B).

consistent with Os-rich, Ru-poor iridium, approximately spanning the range $Ir_{80}Os_{20}$ – $Ir_{65}Os_{35}$.

Compositions (atomic %) of sulfides and alloys are summarized in the Os–Ru–Ir diagram (Fig. 7A). Compositions from the same polyphase inclusion are joined with tie lines, showing the associations Os-rich laurite with erlichmanite (anal. 1401a–2a and 2399b–1, Table 3), Os-rich laurite with Os–Ir alloy (anal. 2375–6, Table 3), and Os-rich erlichmanite with Os–Ir alloy (anal. 2243a–1, Table 3). It is important to note that the last pair forms a continuous trend of compositions along the join Os–Ir of the diagram.

The grains of secondary Ru–Os–Fe oxide

Some grains characterized by a distinct anisotropy and bireflectance were found along cracks in the chromite, associated with chlorite and serpentine. On the basis of their optical and compositional characteristics, they were ascribed to the same species of unknown Ru–Os–Ir–Fe oxide as that reported in the chromitites of Vourinos (Garuti & Zaccarini 1997) and Nurali (Garuti *et al.* 1997). These minerals are believed to originate by *in situ* alteration of laurite crystals, involving progressive loss of S and gain of Fe and O at a relatively low temperature (Garuti & Zaccarini 1997).

The Ir–Rh sulfides, sulfarsenides, and arsenides

Compositions of Ir–Rh sulfides are described in terms of the triangular diagram S – (Ni + Fe + Cu) – (Ir + Rh) (Fig. 7B). They define four main groups, with stoichiometries X_2S_3, X_3S_4, X_9S_8, and $X_{1-x}S$, some of which have (Ir + Rh) > (Ni + Fe + Cu) and correspond to PGM *sensu stricto* already known in the literature, such as kashinite (Begisov *et al.* 1985) and cuproiridsite (Rudashevskii *et al.* 1985a). Others are characterized by prevalence of the base metals over the PGE, and correspond to rhodian pentlandite and unknown Ir–Rh–Ni sulfides.

Kashinite: ideally $(Ir,Rh)_2S_3$

Polygonal, single-phase crystals of kashinite were found enclosed in unaltered chromite. An electron-microprobe analysis carried out on the largest grain (3 × 6 μm) indicates a Rh content up to 5.8 wt%, along with trace amounts of Pt, Ni, and Cu; the stoichiometry corresponds to the formula $(Ir_{1.66}Rh_{0.26}Pt_{0.01}Ni_{0.01}Cu_{0.02})_{\Sigma 1.96}S_{3.04}$ (anal. 1401b–5, Table 4).

Cuproiridsite: ideally $CuIr_2S_4$

Cuproiridsite also occur as solitary inclusions (up to 8 μm) in the same sample of chromite that hosts the kashinite. The grains generally have a shape corresponding to a section through a cubic crystal. The electron-microprobe composition (anal. 1401b–1, Table 4) shows the presence of minor Pt (1.64 wt%), Pd (0.11 wt%) and Ni (0.22 wt%), and can be recalculated to the formula $(Cu_{0.94}Ni_{0.02})_{\Sigma 0.96}(Ir_{1.66}Rh_{0.33}Pt_{0.05})_{\Sigma 2.04}S_4$.

Unknown Ir–Rh–Ni Sulfide

Several grains of an unknown Ir–Rh-bearing sulfide were encountered as constituent of composite inclusions with laurite, characterized by a Ru:Os ratio lower than $Ru_{80}Os_{20}$, erlichmanite, and Rh-rich pentlandite (Figs. 4C, D, 5A, B, C). The mineral is gray-brown to yellow,

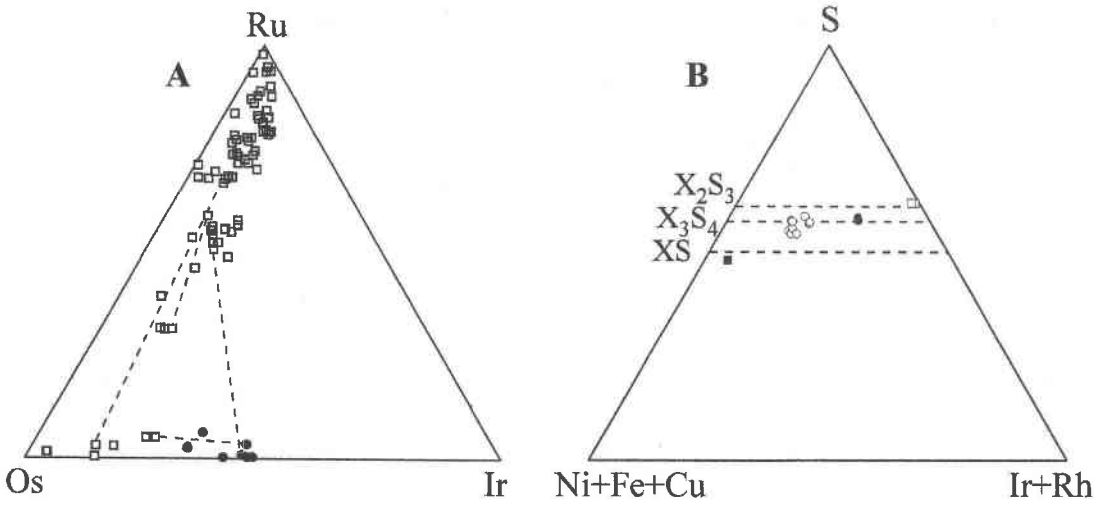

FIG. 7. A) Composition (atom %) of laurite, erlichmanite and Os–Ir alloys in the Os–Ru–Ir ternary system. Tie lines join compositions coexisting in the same composite inclusion. Open squares: laurite–erlichmanite series, filled circles: Os–Ir alloy. B) Composition (atom %) of Ir–Rh sulfides. Open square: kashinite, filled circles: cuproiridsite, open circles: unknown Ir–Rh–Ni sulfide, filled square: rhodian pentlandite.

generally less reflectant than laurite. Optical anisotropy has been observed in some large grains. Electron-microprobe analyses (Table 3) show Ir and Ni as the major constituents, along with minor Rh (0–5.45 wt%), Fe (4.13–7.64%) and Cu (4.12–6.36%). Trace amounts of Ru, Pt and Pd were encountered sporadically. Compositions plotted in the diagram S – (Ni + Fe + Cu) – (Ir + Rh) indicate an intermediate stoichiometry between monosulfide $(Ir>Rh)(Ni>Fe\geq Cu)_2S_3$ and thiospinel $(Ir>Rh)(Ni>Fe\geq Cu)_2S_4$ (Fig. 7B). The mineral is similar to Ir–Rh–Ni–Fe–Cu sulfides reported from other mantle-hosted chromitites in the world, such as Finero (Italy), Ojén (Spain), and Kempirsai (Kazakhstan) (Garuti *et al.* 1995, Melcher *et al.* 1997, Daltry & Wilson 1997).

Rhodian pentlandite

Two grains of rhodian pentlandite were found in fresh chromite, forming composite inclusions, one in association with laurite and Ir–Rh–Ni sulfide (anal. 1400–4, Table 4), the other associated with irarsite (anal. 1400–5, Table 4). In both cases, the pentlandite has a very high Ni:Fe value, and contains up to 8.06 wt% Rh, corresponding to the approximate formula $(Ni_{5.7}Fe_{2.4}Rh_{0.7})_{\Sigma 8.8}S_{8.2}$.

Irarsite: ideally IrAsS

The sulfarsenide irarsite is also a common constituent of the composite PGM inclusions in fresh chromite. The grains range from euhedral laths to anhedral patches usually attached to the external boundary of laurite. A selected electron-microprobe composition (anal. 1400–5, Table 4) indicates that irarsite in primary inclusions differs from irarsite in exsolution-induced blebs in secondary laurite by the presence of substantial Ru (2.51 wt%) substituting for Ir, and the absence of Pt.

Cherepanovite: ideally RhAs

One anisotropic, white to pinkish mineral having the stoichiometry $(Rh_{0.58}Ru_{0.37}Ni_{0.03})_{\Sigma 0.98}$ $(As_{0.99}S_{0.03})_{\Sigma 1.02}$ was found as part of a 10 × 8 μm inclusion composed of irarsite and an unidentified Ru–Os–Rh arsenide. On the basis of an electron-microprobe analysis (anal. 2078–3, Table 4), the mineral can be ascribed to the rare species cherepanovite, although the substantial amount of Ru suggests a broad solid-solution with ruthenarsenite (Ru,Ni)As. Cherepanovite was previously reported from a placer deposit related with the ophiolite belt of Koriakskho–Kamchatskaya, in the eastern Chukot Peninsula of the Russian Far East (Rudashevskii *et al.* 1985b). This probably represents the first occurrence of cherepanovite as an inclusion in chromite.

Unknown $(Rh,Ni)_2As$

The mineral (anal. 2243b–2, Table 4) roughly corresponds to the unreported stoichiometry $(Rh,Ni)_2As$, with minor incorporation of Ir (5.3 wt%) and Ru (6.41 wt%). It occurs as an irregular, porous aggregate adjacent to laurite and clinopyroxene in contact with altered chromite and chromian clinochlore (Fig. 5C). Textural

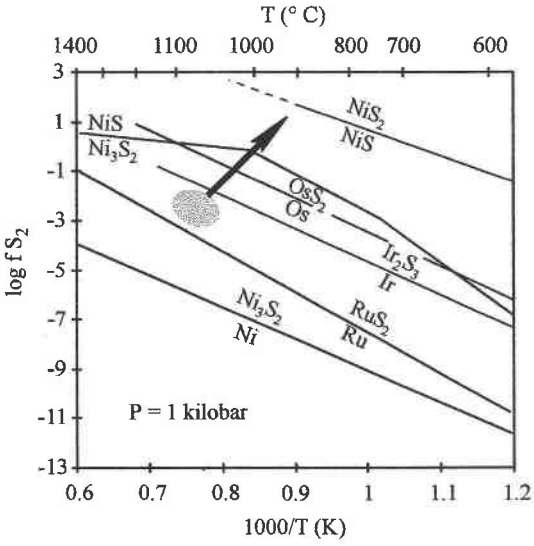

FIG. 8. Metal–sulfide equilibrium curves for Ru, Os, Ir and Ni as function of sulfur fugacity, expressed as log $f(S_2)$, and temperature (T), modified after Melcher *et al.* (1997) and references therein. Dashed field shows conditions prevailing in mantle-hosted chromitites from ophiolite complexes (see Table 5). Arrow indicates the possible trend of $f(S_2)$–T variation at Ray–Iz.

relations indicate that the arsenide probably formed during alteration of the primary PGM inclusion at low temperature.

DISCUSSION

Origin of the primary PGM inclusions

Two major hypotheses have been proposed to explain the occurrence of PGM inclusions in unaltered grains of chromite: i) the PGM inclusions are exsolved from the chromite host at a subsolidus stage, or ii) they are magmatic minerals precipitated early, and mechanically collected on growth surfaces of chromite crystals.

Exsolution of PGM from chromite has long been considered unreliable by many authors because of a number of counter-arguments (Constantinides *et al.* 1980, Talkington *et al.* 1984, Stockman & Hlava 1984, Augé & Johan 1988), but it received some support from experimental works in which PGE (*i.e.*, Ru and Rh) were believed to enter the spinel structure in a true solid-solution (Capobianco & Drake 1990, Capobianco *et al.* 1994). This basic premise, however, has been definitely undermined by the "metal clusters" hypothesis (Tredoux *et al.* 1995), which provided an alternative interpretation of the experimental results. These authors suggested that the fractionation of PGE into spinels may simply reflect physical trapping of submicroscopic clusters of PGE in the metallic state. According to this theory, clusters consisting of a few hundred atoms of the PGE are initially present in a natural chromite-forming system at a high temperature. Because of their physical and chemical properties, the clusters coalescence to form PGM alloys or sulfides, which are subsequently enclosed into early-crystallizing magnesiochromite and silicates (*e.g.*, forsterite). Thereby, the cluster model does not require any crystal-chemical compatibility of individual PGE in favor of the spinel structure, but provides an explanation of the similarity of PGM species (*i.e.,* laurite or Os–Ir alloys) in magnesiochromite and forsterite coexisting in natural chromitites, a feature that strongly argues against PGM exsolution from chromite (Ferrario & Garuti 1990, Garuti & Zaccarini 1997). Preferential precipitation of sulfides *versus* alloys will be controlled by the appropriate $f(S_2)$ prevailing in the melt. In this way, PGE clusters are surrounded and stabilized by S anions and convert into a PGM sulfide on cooling (Tredoux *et al.* 1995).

Sulfur fugacity in the Ray–Iz chromitites

The origin of the primary PGM inclusions in the Ray–Iz chromitites can be modeled by a sequence of events of crystallization controlled by relative stability of PGE alloys and sulfides as function of $f(S_2)$ and T (Fig. 8). The $f(S_2)$ is expected to increase with decreasing T in magmatic systems. The Ru, Ir and Os sulfides become progressively stable over a range of about four log units in $f(S_2)$ at a given temperature, or in a thermal interval of 300–400°C at a constant $f(S_2)$. Thus the final paragenesis (sulfides *versus* alloys) will depend on the initial $f(S_2)$, and the timing of chromite crystallization, which represents the closure of the system in which PGM inclusions are formed. The PGM assemblages at Ray–Iz indicate that $f(S_2)$ was initially as low as to allow the precipitation of Os–Ir alloy, which is interpreted to result from the conversion of refractory Os–Ir clusters. These grains of alloy could coexist with laurite and probably kashinite (Ir_2S_3), which presumably crystallized from Ru–(Os)–S and Ir–Rh–S cluster precursors, respectively. Substitution of Os for Ru in laurite increased with decreasing T, up to the erlichmanite field and across the Os–OsS_2 buffer. Cuproiridsite and the Ir–Rh-bearing Ni–Cu sulfides probably entered their field of stability from this stage up to higher $f(S_2)$ and lower T, which accounts for their exclusive association with erlichmanite or Os-rich laurite. The presence of sulfarsenides and arsenides as primary inclusions attests to an appreciable activity of As in the system at high temperatures. However, the fact that irarsite invariably occurs as small particles attached to the external boundary of the adjacent sulfides suggests a late crystallization, after the sulfides. The buffers Ni_3S_2–NiS and Os–OsS_2 cross each other at about 1050° and 650°C (Fig. 8). In this thermal range, therefore, precipitation

of millerite marks the achievement of the highest $f(S_2)$, the NiS–NiS_2 buffer acting as the upper limit. The absence of the typical sulfide assemblage pyrrhotite, pentandite, chalcopyrite deriving from equilibration of *Mss*, the magmatic monosulfide solid-solution, indicates that sulfur saturation was never reached at Ray–Iz, and thus no immiscible sulfide liquid appeared in the system before the precipitation of chromite. If sulfides can form by reaction of base-metal chlorides or hydroxides with H_2S, as has been proposed by Ballhaus & Stumpfl (1986) and Ferrario & Garuti (1990), the Ni–Cu sulfides commonly attached to the external boundary of PGM-bearing composite inclusions may well have crystallized at temperatures well below the liquidus of the *Mss* (1195–1000°C).

There is evidence that $f(S_2)$ increased sharply in the final stages of PGM precipitation. Patterns of zoning indicate that laurite crystals adjusted their composition in response to the rapid change of thermodynamic conditions. The association of Os–Ir alloy with almost pure OsS_2 is apparently "metastable", and would suggest that pure erlichmanite formed by addition of S and Os to pre-existing Os–Ir alloys, as a consequence of high $f(S_2)$ and low T. This event was followed shortly afterward by the complete crystallization of chromite, which prevented any further re-equilibration of the population of PGM inclusions.

Sulfur fugacity in chromitites of ophiolitic upper mantle

The paragenesis of PGM inclusions from major ore deposits located in the mantle section of ophiolite complexes (Table 5) indicates that the petrogenetic context of podiform chromitites is characterized by extremely low $f(S_2)$, extending to about two log units above the

TABLE 5. MINERALOGY OF PRIMARY PGM INCLUSIONS IN CHROMITE FROM MAJOR CHROMIUM ORE DEPOSITS LOCATED IN THE MANTLE SECTION OF OPHIOLITE COMPLEXES

Complexes	R–I	KEM	VOU	OTH	ALB	TRO	TUR	SAM	ACO	TIE	MAS	TM
Location	U	U	Gr	Gr		Cy		Om	Phl	NC	NC	QC
References	1	2,3	4,5,6,7	8	3,9	3,10,11	5	12	13	5,6,12	5,12	14
Os–Ru–Ir alloys												
Osmium	OOO	OOO	OOO	×	OO		OO		OOO	×	OOO	OO
Iridium	×	OOO	×		O		O			O	O	
Ruthenium					O							
Rutheniridosmine			×									
Ru–Os–(Ir) sulfides												
Laurite	OOO	OOO	OOO	OOO	OOO	OOO	OO	OOO	OOO	OOO	O	OOO
Erlichmanite	OOO	OOO		OO	O	×				OOO		
Ir–Rh sulfides												
Kashinite	O	O			×					OO		
Cuproiridsite	O			×	×					O		
Xingzhongite										×		
un. $(Ir,Rh)(Ni,Cu)_2S_3$	OOO	OOO								×		
un. $(Ir,Rh)(Ni,Cu)_2S_4$	O											
Ruthenian-rhodian pentlandite	O		×		×					O		
Ir–Os–Ru sulfarsenides												
Irarsite	OO		O									
Osarsite			O									
Ruarsite												
Arsenides												
Cherepanovite	×											
Pt–Pd PGM												
Cooperite						×						
Sperrylite				×								

OOO: very abundant, OO: major, O: minor, ×: very rare, un.: unknown. Complexes: R–I: Ray–Iz, KEM: Kempirsay, VOU: Vourinos, OTH: Othrys, ALB: Albania, TRO: Troodos, TUR: Turkey, SAM: Samail, ACO: Acoje, TIE: Tiebaghi, MAS: Massif du Sud, TM: Thetford Mines. Location: U: Urals, Gr: Greece, Cy: Cyprus, Om: Oman, Phl: Philippines, NC: New Caledonia, QC: Quebec. References: 1) this work, 2) Melcher *et al.* (1997), 3) unpubl. data of the authors, 4) Augé (1985), 5) Legendre & Augé (1986), 6) Augé (1988), 7) Garuti & Zaccarini (1997), 8) Garuti *et al.* (1999), 9) Ohnenstetter *et al.* (1991), 10) Constantinides *et al.* (1980), 11) McElduff & Stumpfl (1990), 12) Augé & Johan (1988), 13) Orberger *et al.* (1988), 14) Corrivaux & Laflamme (1990).

equilibrium Ru–RuS_2, thus keeping well below the Os–OsS_2 buffer in most cases. The study of PGM nuggets from ophiolite-related placer deposits suggests that, in some cases, the $f(S_2)$ did not even exceed the Ru–RuS_2 reaction boundary, and only Ru-rich alloys in the Os–Ir–Ru ternary system were able to crystallize (Nakagawa & Franco 1997, and reference therein). At the low $f(S_2)$ (and high T) prevailing in most ophiolitic chromitites, however, laurite coexists with Os–Ir alloy, and its composition remains strictly confined within the range Ru_{100}–$Ru_{72}Os_{28}$, the latter corresponding to the Ru:Os atomic ratio in the C1 chondrite (Fig. 9). The $(Ru,Os)S_2$ + OsS_2 assemblage reported from the Othrys ophiolite suggests that $f(S_2)$ was initially sufficiently high to cause laurite characterized by the chondritic Ru:Os ratio (Fig. 9) to be the first PGM to crystallize (Garuti *et al.* 1999), and that $f(S_2)$ increased to attain the Os–OsS_2 buffer, although it probably did not exceed this limit significantly. The presence of monomineralic laurite in chromite (Samail, Troodos) is consistent with intermediate $f(S_2)$ and T, but at the same time it is consistent with even more restricted ranges of variation of $f(S_2)$ (Augé & Johan 1988). The appearance of abundant erlichmanite and Ir–Rh sulfides in the PGM assemblage marks a limit of $f(S_2)$ that is rarely exceeded in chromitites hosted in the ophiolitic upper mantle. The only examples appear to be those of Kempirsai, Tiebaghi, and Ray–Iz (Table 5), and consistently, the Os content of laurite in chromitites from these complexes exceeds the chondritic composition, entering the field of erlichmanite (Figs. 7 and 9A, B). The paragenetic assemblage of PGM and the compositional variation of laurite suggest that $f(S_2)$ was initially sufficiently low to enable precipitation of Ru-rich laurite as the only sulfide phase coexisting with the Os–Ir alloy, but it increased by at least four log units, reaching the stability field of erlichmanite and Ir–Rh-bearing sulfides in the final stages. The thermal interval probably spans more than 250°C, indicating that PGM and chromite crystallization proceeded down to much lower temperatures compared with the situation in other ophiolite complexes. Such low temperatures are incompatible with the anhydrous nature of the relevant magma. The stability of chromite in hydrous systems is poorly constrained on the basis of experiments; we can expect the temperature of chromite crystallization to be lowered by the presence of an aqueous fluid phase in the system (Johan *et al.* 1983). Thermal conditions estimated from the olivine–chromite equilibrium and presence of primary inclusions of chlorite at Ray–Iz suggest that the onset of chromite precipitation may have been displaced down to temperatures well below 1000°C, resulting in a relative increase of $f(S_2)$ in the system, which was recorded in the PGM assemblage and composition of laurite inclusions. The presence of disequilibrium associations in composite PGM inclusions, as well as the patterns of

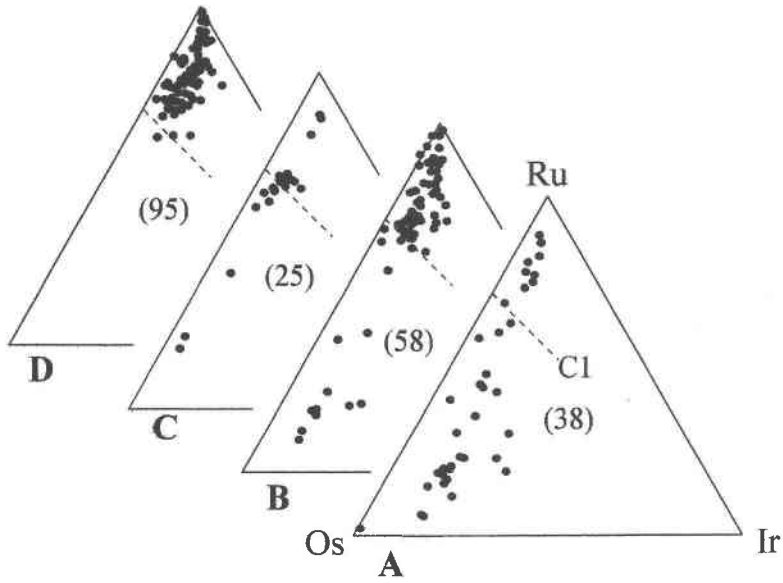

FIG. 9. Composition of PGM of the laurite–erlichmanite series included in mantle-hosted chromitites from various ophiolite complexes. A) Kempirsai (southern Urals), B) Tiebaghi (New Caledonia), C) Othrys (Greece), D) Vourinos (Greece), Troodos (Cyprus), Samail (Oman); C1: Os–Ru atomic proportion in chondrite. The number of compositions plotted is shown in brackets. See Table 5 for the sources of data.

zonation of some laurite grains from Ray–Iz, indicate that the early-crystallized, high-T PGM underwent partial to total re-equilibration in response to increasing $f(S_2)$ and decreasing T.

Conclusions

1) The present study has confirmed that chromitite samples from Ray–Iz contain laurite characterized by a wide range of Ru–Os–Ir substitution, as previously reported by Anikina *et al.* (1996). In addition, it has revealed that laurite is accompanied by a great variety of Os–Ir–Rh sulfides, which are indicators of relatively low T and high $f(S_2)$.

2) Such a complexity of the PGM assemblage is unusual compared with PGM associations in mantle-hosted chromitites of other ophiolite massifs. It apparently characterizes those chromitites (Kempirsai, Ray–Iz, Tiebaghi) that formed in the ophiolitic upper mantle under exceptionally high activity of fluids, causing crystallization of PGM and chromite to proceed down to low T, under relatively high $f(S_2)$.

3) It has been shown that the giant chromite orebodies of Kempirsai formed or recrystallized by interaction of residual mantle with volatile-rich alkali-bearing fluids, following the development of an intraoceanic subduction zone east of the European plate, during Devonian times (Melcher *et al.* 1997, and references therein). Petrological and structural analogies indicate that fluid-induced metasomatism occurred even in the residual oceanic mantle of the Polar Urals, and was probably responsible for the formation and re-equilibration of the chromite–PGM system at Ray–Iz.

Acknowledgements

The authors thank Fernando Bea for having made available the facilities of the Electron Microscopy Laboratory at the University of Granada (Spain), and Isabel Guerra for her help in obtaining the BSE images used in this work. The Italian National Research Council (CNR) is acknowledged for financing the electron-microprobe laboratory at the Department of Earth Sciences of the University of Modena. The manuscript was improved by the constructive criticisms by Mitsuru Nakagawa, Geological Survey of Japan, Thierry Augé, BRGM, and the thorough editorial review of Robert Martin.

References

Anikina, Y.V., Moloshag, V.P., Alimov, V.Y. & Kononkova, N.N. (1996): Type chemistry of laurite from Polar Ural Alpine-type hyperbasites. *Dokl. Russ. Acad. Sci., Earth-Sci. Sect.* **345**, 410-412.

Augé, T. (1985): Platinum-group-mineral inclusions in ophiolitic chromitite from the Vourinos Complex, Greece. *Can. Mineral.* **23**, 163-171.

_____ (1988): Platinum-group minerals in the Tiébaghi and Vourinos ophiolitic complex: genetic implications. *Can. Mineral.* **26**, 177-192.

_____ & Johan, Z. (1988): Comparative study of chromite deposits from Troodos, Vourinos, North Oman and New Caledonia ophiolites. *In* Mineral Deposits within the European Community (J. Boissonnas & P. Omenetto, eds.). Springer, Berlin, Germany (267-288).

Ballhaus, C.G. & Stumpfl, E.F. (1986): Sulfide and platinum mineralization in the Merensky Reef: evidence from hydrous silicates and fluid inclusions. *Contrib. Mineral. Petrol.* **94**, 193-204.

Begisov, V.D., Zav'yalov, E.N., Rudashevskii, N.S. & Vyal'sov, L.N. (1985): Kashinite $(Ir,Rh)_2S_3$ – a new sulfide of iridium and rhodium. *Zap. Vses. Mineral. Obshchest.* **114**, 617-622 (in Russ.).

Capobianco, C.J. & Drake, M.J. (1990): Partitioning of ruthenium, rhodium, and palladium between spinel and silicate melt and implications for platinum group element fractionation trends. *Geochim. Cosmochim. Acta* **54**, 869-874.

_____, Hervig, R.L. & Drake, M.J. (1994): Experiments on crystal/liquid partitioning of Ru, Rh and Pd for magnetite and hematite solid solutions crystallized from silicate melt. *Chem. Geol.* **113**, 23-43.

Constantinides, C.C., Kingston, C.A. & Fisher, P.C. (1980): The occurrence of platinum group minerals in the chromitites of the Kokkinorotsos chrome mine, Cyprus. *In* Ophiolites, Proc. of the Int. Ophiolite Symp. (Cyprus, 1979; A. Panayiotou, ed.). Geol. Survey Dep., Nicosia, Cyprus (93-101).

Corrivaux, L. & Laflamme, J.H.G. (1990): Minéralogie des éléments du groupe du platine dans les chromitites de l'ophiolite de Thetford Mines, Québec. *Can. Mineral.* **28**, 579-595.

Daltry, V.D.C. & Wilson, A.H. (1997): Review of platinum-group mineralogy: compositions and elemental associations of the PG-minerals and unidentified PGE-phases. *Mineral. Petrol.* **60**, 185- 229.

Efimov, A.A., Lennych, V.I., Puchkov, V.N., Savelyev, A.A., Savelyeva, G.N. & Yazeva, R.G. (1978): Guidebook for the excursion "Ophiolites of the Polar Urals". *In* Fourth Field Ophiolite Conf. (N.A. Bogdanov, ed.). Institute of Geology, Academy of Sciences of USSR, Moscow, Russia.

Fawcett, J.J. & Yoder, H.S., Jr. (1966): Phase relationships of chlorites in the system $MgO–Al_2O_3–SiO_2–H_2O$. *Am. Mineral.* **51**, 353-380.

Ferrario, A. & Garuti, G. (1990): Platinum-group mineral inclusions in chromitites of the Finero mafic–ultramafic complex (Ivrea-Zone, Italy). *Mineral. Petrol.* **41**, 125-143.

GARUTI, G., GAZZOTTI, M. & TORRES-RUIZ, J. (1995): Iridium, rhodium and platinum sulfides in chromitites from the ultramafic massifs of Finero, Italy, and Ojén, Spain. *Can. Mineral.* **33**, 509-520.

_____ & ZACCARINI, F. (1997): *In situ* alteration of platinum-group minerals at low temperature: evidence from serpentinized and weathered chromitite of the Vourinos complex, Greece. *Can. Mineral.* **35**, 611-626.

_____, _____, CABELLA, R. & FERSHTATER, G. (1997): Occurrence of unknown Ru–Os–Ir–Fe oxide in the chromitites of the Nurali ultramafic complex, southern Urals, Russia. *Can. Mineral.* **35**, 1431-1440.

_____, _____ & ECONOMOU-ELIOPOULOS, M. (1999): Paragenesis and composition of laurite from chromitites of Othrys (Greece): implications for Os–Ru fractionation in ophiolitic upper mantle of the Balkan peninsula. *Mineral. Deposita* **34**, 312-319.

JOHAN, Z., DUNLOP, H., LE BEL, L., ROBERT, J.-L. & VOLFINGER, M. (1983): Origin of chromite deposits in ophiolitic complexes: evidence for a volatile- and sodium-rich reducing fluid phase. *Fortschr. Mineral.* **61**, 105-107.

HARRIS, D.C. & CABRI, L.J. (1991): Nomenclature of platinum-group-element alloys: review and revision. *Can. Mineral.* **29**, 231-237.

KOROTEEV, V.A., DE BOORDER, H., NECHEUKHIN, V.M. & SAZONOV, V.N. (1997): Geodynamic setting of the mineral deposits of the Urals. *Tectonophys.* **276**, 291-300.

LEGENDRE, O. & AUGÉ, T. (1986): Mineralogy of platinum-group mineral inclusions in chromitites from different ophiolitic complexes. *In* Metallogeny of the Basic and Ultrabasic Rocks (M.J. Gallagher, R.A. Ixer, C.R. Neary & H.M. Prichard, eds.). The Institute of Mining and Metallurgy, London, U.K. (361-372).

MAKEYEV, A.B., PEREVOZCHIKOV, B.V. & AFANASYEV, A.K. (1985): *Chromite in the Polar Urals.* Komi Branch of the Academy of Sciences of USSR, Siktivar, Russia (in Russ.).

MCELDUFF, B. & STUMPFL, E.F. (1990): Platinum-group minerals from the Troodos ophiolite complex, Cyprus. *Mineral. Petrol.* **42**, 211-232.

MELCHER, F., GRUM, W., SIMON, G., THALHAMMER, T.V. & STUMPFL, E.F. (1997): Petrogenesis of the ophiolitic giant chromite deposits of Kempirsai, Kazakhstan: a study of solid and fluid inclusions in chromite. *J. Petrol.* **38**, 1419-1458.

NAKAGAWA, M. & FRANCO, H.E.A. (1997): Placer Os–Ir–Ru alloys and sulfides: indicators of sulfur fugacity in an ophiolite? *Can. Mineral.* **35**, 1441-1452.

OHNENSTETTER, M., KARAJ, N., NEZIRAJ, A., JOHAN, Z. & CINA, A. (1991): Le potentiel platinifère des ophiolites: minéralisations en éléments du groupe du platine (PGE) dans les massifs de Tropoja et Bulqiza, Albanie. *C.R. Acad. Sci. Paris* **313**, *Sér.* **II**, 201-208.

ORBERGER, B., FRIEDRICH, G. & WOERMANN, E. (1988): Platinum-group element mineralization in the ultramafic sequence of the Acoje ophiolite block, Zambales, Philippines. *In* Geoplatinum 87 (H.M. Prichard, J. Potts, J.F.W. Bowles & S.J. Cribb, eds.). Elsevier, Amsterdam, The Netherlands (361-380).

PEREVOZCHIKOV, B.V., ALIMOV, V.YU., TSARITSIN, YE.P., CHASHCHUKHIN, I.S. & SHERSTOBITOVA, L.A. (1990b): Chrome spinels and chromite ore deposits of the massif. *In* Structure, Evolution and Minerogenesis of the Ray–Iz Ultramafic Massif. The Ural Branch of the Academy of Sciences of USSR, Sverdlovsk, Russia (149-194; in Russ.).

_____, CHASHCHUKHIN, I.S. & TSARITSIN, YE.P. (1990a): Metamorphism of the ultramafic massif and its supposed primary composition. *In* Structure, Evolution and Minerogenesis of the Ray–Iz Ultramafic Massif. The Ural Branch of the Academy of Sciences of USSR, Sverdlovsk, Russia (29-57; in Russ.).

_____ & PUCHKOV, V.N. (1990): Geologic structure of the massif. *In* Structure, Evolution and Minerogenesis of the Ray–Iz Ultramafic Massif. The Ural Branch of the Academy of Sciences of USSR, Sverdlovsk, Russia (19-28; in Russ.).

RUDASHEVSKII, N.S., MEN'SHIKOV, YU.P., MOCHALOV, A.G. TRUBKIN, N.V., SHUMSKAYA, N.I. & ZHDANOV, V.V. (1985a): Cuprorhodsite, $CuRh_2S_4$, and cuproiridsite, $CuIr_2S_4$, new natural thiospinels of platinum-group elements. *Zap. Vses. Mineral. Obshchest.* **114**(2), 187-195 (in Russ.).

_____, MOCHALOV, A.G., TRUBKIN, N.V., SHUMSKAYA, N.I., SHKURSKY, V.I. & EVSTIGNEEVA, T.L. (1985b): Cherepanovite, RhAs, a new mineral. *Zap. Vses. Mineral. Obshchest.* **114**, 464-469 (in Russ.).

SACK, R.O. & GHIORSO, M.S. (1991): Chromian spinels as petrogenetic indicators: thermodynamics and petrological applications. *Am. Mineral.* **76**, 827-847.

SAVEL'YEV, A.A. & SAVEL'YEVA, G.N. (1977): Ophiolites of the Voykar–Syn'insk massif (Polar Urals). *Geotectonics* **11**, 427-437.

SHMELEV, V.P., GONCHARENKO, A.I., CHERNYSHEV, A.I., PUCHKOV, V.N. & PEREVOZCHIKOV, B.V. (1990): Tectonics of ultramafic and gabbroic rocks. *In* Structure, Evolution and Minerogenesis of the Ray–Iz Ultramafic Massif. The Ural Branch of the Academy of Sciences of USSR, Sverdlovsk, Russia (88-148; in Russ.).

SOBOLEV, V.S. & DOBRETSOV, N.L. (1977): Petrology and metamorphism of ancient ophiolites – an examples of the Polar Urals and West Sayan. *Trans. Inst. Geol. Geophys.* **368**, 217 p. (in Russ. with extended abstr. in English). Siberian Branch of the Academy of Sciences of the USSR.

SPRINGER, R.K. (1974): Contact metamorphosed ultramafic rocks in the western Sierra Nevada Foothills, California. *J. Petrol.* **15**, 160-195.

STOCKMAN, H.W. & HLAVA, P.F. (1984): Platinum-group minerals in Alpine chromitites from southwestern Oregon. *Econ. Geol.* **79**, 491-508.

TALKINGTON, R.W., WATKINSON, D.H., WHITTAKER, P.J. & JONES, P.C. (1984): Platinum-group mineral and other solid inclusions in chromite of ophiolitic complexes: occurrence and petrological significance. *Tschermaks Mineral. Petrogr. Mitt.* **32**, 285-301.

TREDOUX, M., LINDSAY, N.M., DAVIES, G. & MACDONALD, I. (1995): The fractionation of platinum-group elements in magmatic systems, with the suggestion of a novel causal mechanism. *S. Afr. J. Geol.* **98**, 157-167.

VOLCHENKO, YU.A. (1990): Geochemistry and mineralogy of platinoids and gold in the ultramafic rocks and chromite ores. *In* Structure, Evolution and Minerogenesis of the Ray–Iz Ultramafic Massif. The Ural Branch of the Academy of Sciences of USSR, Sverdlovsk, Russia (195-206; in Russ.).

Received January 8, 1999, revised manuscript accepted August 4, 1999.